

Electroweak boson production at LHCb

Jonathan Anderson^{*†}

Physik-Institut der Universität Zürich, Switzerland.

E-mail: jonathan.anderson@cern.ch

The electroweak boson production cross-sections have been measured in the forward region using $\sqrt{s} = 7$ TeV proton-proton collision data recorded at the LHCb experiment. The inclusive W measurement is performed in the $W \rightarrow \mu\nu$ channel while the inclusive Z measurement has been made using di-muon, di-electron, and di-tau final states. The associated production of Z bosons and jets has been measured for final states where the Z decays to a dimuon pair. The Drell-Yan production cross-section below the Z peak has been measured using di-muons with invariant masses down to 5 GeV. All of these measurements are found to be in agreement with NLO or NNLO QCD predictions.

*36th International Conference on High Energy Physics,
July 4-11, 2012
Melbourne, Australia*

^{*}Speaker.

[†]on behalf of the LHCb collaboration

1. Introduction

The LHCb [1] detector, one of the four large experiments at the Large Hadron Collider (LHC), is a forward single-arm spectrometer that is fully instrumented with calorimeter, tracking, and particle identification detectors in the pseudorapidity range $2 < \eta < 5$. Although primarily designed to study heavy flavour physics, LHCb is capable of making precision electroweak boson measurements in the forward region. Since the pseudorapidity range $2.5 < \eta < 5$ is unique to LHCb, these measurements are complementary to the electroweak boson measurements from ATLAS and CMS, which have full coverage for $|\eta| < 2.5$. This contribution describes the following measurements that have been made using proton-proton collision data at $\sqrt{s} = 7$ TeV recorded by the LHCb detector: $W \rightarrow \mu\nu$ and $Z \rightarrow \mu\mu$ production and their ratios and asymmetries [2], $Z \rightarrow ee$ production [3], $Z \rightarrow \tau\tau$ production [4], the associated production of jets and Z bosons [5], and the production of Drell-Yan dimuon pairs down to invariant masses of 5 GeV [6]. In all cases the cross-sections are measured in a fiducial region where the final state leptons and jets are required to have pseudorapidities in the range $2 < \eta < 4.5$.

These measurements constitute an important test of Quantum Chromodynamics (QCD) and provide useful information on the parton distribution functions (PDFs) describing the internal structure of the proton. For electroweak boson production at LHCb, the momenta of the two interacting partons are highly asymmetric, meaning that events at LHCb simultaneously probe a region at high- x and a region at low- x , where the uncertainties on the proton PDFs are relatively large. Theoretical predictions of the electroweak boson production cross-sections at the LHC are made by convoluting the partonic level cross-section and the proton PDFs. While electroweak theory can currently describe the fundamental partonic processes for W and Z production at next-to-next-to-leading order (NNLO) with an accuracy at the percent level, an uncertainty of 3-10% arises from the present knowledge of the proton PDFs. The uncertainty on both the partonic cross-section and the PDFs increase substantially for Drell-Yan production below the Z mass. For Drell-Yan events at LHCb with dimuon invariant masses of 5 GeV, bjorken- x values down to 8×10^{-6} are probed and the uncertainties on theoretical predictions are of the order of 50%.

2. Inclusive W and Z production

The inclusive W production cross-section has been measured using the channel $W \rightarrow \mu\nu$ [2] while the inclusive Z measurement was made using the decay modes $Z \rightarrow \mu\mu$ [2], $Z \rightarrow ee$ [3], and $Z \rightarrow \tau\tau$ [4]. In all cases the candidate events were triggered by either a single muon line with a transverse momentum, p_T , threshold of 10 GeV or a single electron line with a p_T threshold of 15 GeV.

Using a dataset with an integrated luminosity of 37.1 pb^{-1} , W candidates are selected by requiring an isolated muon with a $p_T > 20$ GeV lying within $2 < \eta < 4.5$. In order to reduce background contamination, additional criteria are imposed on: the muon impact parameter with respect to the primary vertex, $IP < 40 \mu\text{m}$; the muon isolation within the event; and the requirement that there are no other muons in the event with $p_T > 2$ GeV. The following specific backgrounds are considered: $Z \rightarrow \mu\mu$ events where one of the muons goes outside of the LHCb acceptance; $W \rightarrow \tau\nu$ and $Z \rightarrow \tau\tau$ where one tau decays to a muon inside the detector; semi-leptonic decays of

heavy flavour hadrons; and generic hadronic (QCD) events where kaons or pions are mis-identified as muons due to decay in flight or punch-through. The signal purity is estimated by fitting the muon p_T spectrum to the shapes expected for signal and each background category in 5 bins of the muon pseudorapidity. The background shapes used in the fits are taken either from data or simulation while the shapes of the W^+ and W^- signal distributions are taken from the POWHEG [7] next-to-leading order (NLO) calculation. The fit is performed for both charges and over all pseudorapidity bins simultaneously. The dominant background is due to pion and kaon decays in flight. 15608 W^+ and 12301 W^- candidates are selected with sample purities determined to be 80% and 78%, respectively. The efficiency of the offline $W \rightarrow \mu\nu$ selection is determined from data using offline selected $Z \rightarrow \mu\mu$ events where one of the muons is ignored. Depending on the pseudorapidity bin in question, an efficiency of between 45% and 80% is measured.

$Z \rightarrow \mu\mu$ candidates are identified offline by requiring a pair of oppositely charged muons which combine to a dimuon invariant mass in the range $60 \leq M_{\mu\mu} \leq 120$ GeV. Both muons are required to have p_T larger than 20 GeV and pseudorapidities between 2 and 4.5. Using a dataset corresponding to an integrated luminosity of 37.1 pb^{-1} , 1966 Z candidates are identified. The backgrounds considered are from $Z \rightarrow \tau\tau$ events where both tau leptons decay to muons, heavy flavor decays with two semi-leptonic muonic decays, and generic QCD events where pions or kaons either decay in flight to muons, or punch through the detector and are falsely identified. The selected sample is estimated to have a purity of 99.7%.

The $Z \rightarrow ee$ analysis was performed using a dataset with an integrated luminosity of 945 pb^{-1} . Candidate events are selected offline if they contain two identified electrons with p_T greater than 20 GeV and pseudorapidities in the range $2 < \eta < 4.5$. Due to saturation of the electromagnetic calorimeter and incomplete Bremsstrahlung recovery, the $Z \rightarrow ee$ mass peak is spread to lower values, and so the mass window is chosen to be $M_{ee} > 40$ GeV. The backgrounds considered are $Z \rightarrow \tau\tau$ where both tau leptons decay to electrons, and generic QCD events. In total, 21535 events are selected with an estimated purity of 97.8%.

$Z \rightarrow \tau\tau$ events are identified by requiring two oppositely-charged tracks originating from separate tau decays that are consistent with an electron, muon, or hadron hypothesis, and that have large impact parameters with respect to the primary vertex of the event. Using a dataset corresponding to an integrated luminosity of 1 fb^{-1} , $Z \rightarrow \tau\tau$ events are identified using five different final state combinations, $\mu\mu$, μe , $e\mu$, μh , and eh . These candidates are required to contain either a muon or an electron that has passed the appropriate single lepton trigger line and is reconstructed offline with a p_T greater than 20 GeV and pseudorapidity between 2 and 4.5. The final state is also required to contain a second track that: has a p_T greater than 5 GeV; a pseudorapidity in the range $2 < \eta < 4.5$; is identified as either a muon, electron or hadron; and combines with the triggered lepton to give a di-track invariant mass above 20 GeV. A variety of different QCD and electroweak backgrounds have been evaluated. In total, for the five modes combined, 990 candidates are selected with a purity between 60 and 75%, depending on the mode. In order to compare directly to the $Z \rightarrow \mu\mu$ and $Z \rightarrow ee$ measurements, the results are quoted in the same kinematic region, requiring both taus to be within pseudorapidities of 2 and 4.5, to have transverse momenta above 20 GeV, and an invariant mass between 60 and 120 GeV. Since we actually measure the decay products of the taus and do not detect them directly, an acceptance factor, A , is required. This number has been evaluated using PYTHIA [8] and HERWIG [9], with the difference being taken as a systematic

uncertainty.

The experimental efficiencies for triggering, reconstructing and identifying high p_T muons and electrons have been determined using a "tag and probe" approach and offline selected data samples of $Z \rightarrow \mu\mu$ and $Z \rightarrow ee$ events. Two methods are used to determine the integrated luminosity, a Van der Meer scan [10] and a beam gas method [11]. Both methods give similar results and have a precision of 3.5%. The cross-section results are presented in Figure 1. No corrections are yet applied for final state radiation. All results are consistent with the theoretical predictions calculated using DYNNLO [12] at NNLO and a number of different PDF sets. The $Z \rightarrow \mu\mu$ measurement is limited by the statistical determination of the efficiencies using the 2010 data, with $Z \rightarrow \tau\tau$ limited by statistics, and the $W \rightarrow \mu\nu$ and $Z \rightarrow ee$ measurements are limited by the precision of the luminosity determination.

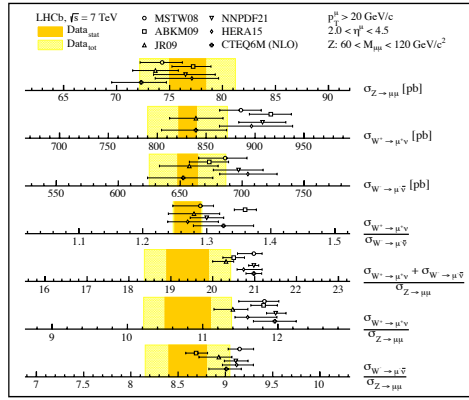


Figure 1: Summary of the W and Z cross-section and ratio measurements. The orange bands correspond to the statistical uncertainties, the yellow band to the statistical and systematic uncertainties added in quadrature. Superimposed are NNLO predictions from DYNNLO with the MSTW08, NNPDF, CTEQ, ABKM, JR and HERA PDF sets.

3. Associated production of Z bosons and jets

The associated production of QCD jets and $Z \rightarrow \mu\mu$ events has been measured using a dataset corresponding to an integrated luminosity of 1 fb^{-1} [5]. The Z bosons are selected using the same criteria as for the inclusive measurement while the jets are reconstructed using the particle flow method and the anti-kt algorithm [13] with the size $R = 0.5$. The jets are required to have p_T greater than 10 GeV and pseudorapidities in the range $2 < \eta < 4.5$. The sample purity is above 99% and is consistent with the purity of the inclusive sample. The jet energy correction has been determined from simulation. The validity of the Z+jet simulation has been investigated using events containing a Z boson and a single jet. The simulation was found to be in good agreement with the data. In order to minimize systematic uncertainties, the measured cross-sections are normalized to the measured inclusive $Z \rightarrow \mu\mu$ cross-section.

The measured cross-section is in good agreement with the NNLO predictions from FEWZ [14]. Figure 2(a) shows the measured cross-section as a function of the Z boson rapidity.

4. Low mass Drell-Yan production

Using a dataset with an integrated luminosity of 37.1 pb^{-1} , the Drell-Yan production cross-section has been measured using dimuons with invariant masses between 5 GeV and 120 GeV [6]. Candidate events are selected via a dimuon trigger and an offline selection that requires that each muon has momenta $p > 10 \text{ GeV}/c$, transverse momenta $p_T > 3 \text{ GeV}/c$, and pseudorapidity $2 < \eta < 4.5$. The mass range $9 < M_{\mu\mu} < 10.5 \text{ GeV}/c^2$, where the $\Upsilon \rightarrow \mu\mu$ contribution dominates, is excluded. While the high mass region at the Z peak is very pure, the background increases significantly towards low masses. Four sources of background have been evaluated: semileptonic heavy flavor decays; pions and kaons that have been mis-identified as muons; $\gamma^*/Z \rightarrow \tau\tau$ events where both taus decay to muons; and, for the mass bins below $10 \text{ GeV}/c^2$, the contribution due to the radiative tail of $\Upsilon \rightarrow \mu\mu$ events.

The signal yield is extracted by a template fit to the minimum muon isolation distribution of the two muons. Here the muon isolation is defined as the fraction of the transverse momenta of the muon-jet carried by the muon, $z = p_T^\mu / p_T^{\text{jet}}$. The muon-jet is defined as the jet which contains the muon, and is reconstructed with the anti-kt algorithm [13] with the size $R = 0.5$. Signal events are expected to have an isolation distribution close to unity while the background events tend to have lower values since they are usually produced in the same direction as the other fragmentation products. Fits are performed in nine different mass and rapidity bins. The signal template used in the fits is obtained from simulation. This is validated by comparing the isolation distribution for $\Upsilon \rightarrow \mu\mu$ and $Z \rightarrow \mu\mu$ events in data and simulation where good agreement is seen. The background templates, describing hadron mis-identification and semi-leptonic heavy flavor decays, are taken from data. The extracted sample purity varies between 7% and 100% depending on the mass and rapidity bin. The uncertainty due to the template shapes is estimated by using templates from independent sources. Here the largest uncertainty is due to the shape of the heavy quark template and varies depending on the mass bin, being 24% in the lowest mass bin and less than 1% for masses above $20 \text{ GeV}/c^2$.

The experimental efficiencies are determined from data. Aside from the uncertainty on the template shapes, the systematic uncertainty is dominated by the uncertainty on the tracking efficiencies which is limited by the available statistics and varies between 4% and 10% depending on the mass and rapidity bin. No corrections are yet applied for final state radiation. Figure 2(b) shows the differential cross-section as a function of the invariant mass of the dimuons together with predictions from PYTHIA [8] (normalised to the cross-section measured in the highest mass bin) and NLO calculations. NLO predictions are only available for FEWZ [14] for masses larger than $7 \text{ GeV}/c^2$ and for DYNNLO [12] for masses larger than $12.5 \text{ GeV}/c^2$. The measured values are in agreement with the NLO predictions.

5. Summary

The inclusive W, Z and low mass Drell-Yan production cross-sections, and the associated production of jets and Z bosons, have been measured in the forward region using $\sqrt{s} = 7 \text{ TeV}$ proton-proton collision data collected by the LHCb experiment. The measured values are in good agreement with NLO or NNLO predictions.

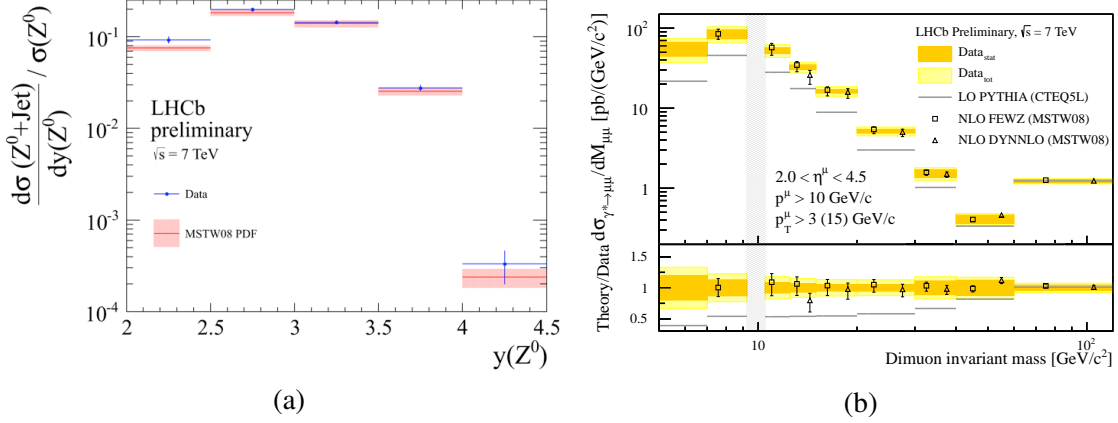


Figure 2: (a) Comparison of the measured Z+jet cross-section as a function of the Z boson rapidity with the NNLO prediction from FEWZ. (b) The measured Drell-Yan cross section as a function of dimuon mass. Superimposed are the PYTHIA predictions and the NLO predictions from FEWZ and DYNNLO. The lower plot shows the ratio of the predictions or the uncertainties to the data

References

- [1] The LHCb collaboration, *The LHCb Detector at the LHC*, JINST **3** S08005 (2008).
- [2] The LHCb collaboration, *Inclusive W and Z production in the forward region at $\sqrt{s} = 7$ TeV*, JHEP **1206**, 058 (2012).
- [3] The LHCb collaboration, *Measurement of the cross-section for $Z \rightarrow ee$ production in pp collisions at $\sqrt{s} = 7$ TeV*, LHCb-CONF-2012-011 (2012).
- [4] The LHCb collaboration, *A study of the Z production cross-section in pp collisions at $\sqrt{s} = 7$ TeV using tau final states*, submitted to JHEP, arXiv:1210.6289v1 [hep-ex] (2012).
- [5] The LHCb collaboration, *Measurement of jet production in $Z \rightarrow \mu\mu$ events at LHCb in $\sqrt{s} = 7$ TeV pp collisions*, LHCb-CONF-2012-016 (2012).
- [6] The LHCb collaboration, *Inclusive low mass Drell-Yan production in the forward region at $\sqrt{s} = 7$ TeV*, LHCb-CONF-2012-013 (2012).
- [7] S. Alioli, P. Nason, C. Oleari and E. Re, JHEP **0807** (2008) 060.
- [8] T. Sjöstrand et. al., Computer Phys. Commun. **135** (2001) 238.
- [9] M. Bahr et. al., "Herwig++ Physics and Manual", Eur. Phys. J. C **58**:639-707, (2008).
- [10] S. van der Meer, *Calibration of the effective beam height in the ISR*, ISR-PO/68-31, 1968.
- [11] The LHCb collaboration, R. Aaij et al., *Absolute luminosity measurements with the LHCb detector at the LHC*, JINST **7** (2012) P01010, arXiv:1110.2866.
- [12] S. Catani, L. Cieri, G. Ferrera, D. de Florian, M. Grazzini, Phys. Rev. Lett. **103** (2009) 082001, arXiv:0903.2120.
- [13] M. Cacciari and G. P. Salam, Dispelling the N3 myth for the k(t) jet-finder, Phys. Lett. B **641** (2006) 57, arXiv:hep-ph/0512210.
- [14] R. Gavin, Y. Li, F. Petriello, and S. Quackenbush, FEWZ 2.0: A code for hadronic Z production at next-to-next-to-leading order, Comput. Phys. Commun. **182** (2011) 2388, arXiv:1011.3540.